

# ReferDINO: Referring Video Object Segmentation with Visual Grounding Foundations

Tianming Liang<sup>1</sup> Kun-Yu Lin<sup>2</sup> Chaolei Tan<sup>3</sup> Jianguo Zhang<sup>4</sup> Wei-Shi Zheng<sup>1</sup> Jian-Fang Hu<sup>1\*</sup>

<sup>1</sup>Sun Yat-sen University <sup>2</sup>The University of Hong Kong

<sup>3</sup>The Hong Kong University of Science and Technology

<sup>4</sup>Southern University of Science and Technology

liangtm@mail2.sysu.edu.cn, hujf5@mail.sysu.edu.cn

## Abstract

Referring video object segmentation (RVOS) aims to segment target objects throughout a video based on a text description. Despite notable progress in recent years, current RVOS models remain struggle to handle complicated object descriptions due to their limited video-language understanding. To address this limitation, we present **ReferDINO**, an end-to-end RVOS model that inherits strong vision-language understanding from the pretrained visual grounding foundation models, and is further endowed with effective temporal understanding and object segmentation capabilities. In ReferDINO, we contribute three technical innovations for effectively adapting the foundation models to RVOS: 1) an object-consistent temporal enhancer that capitalizes on the pretrained object-text representations to enhance temporal understanding and object consistency; 2) a grounding-guided deformable mask decoder that integrates text and grounding conditions to generate accurate object masks; 3) a confidence-aware query pruning strategy that significantly improves the object decoding efficiency without compromising performance. We conduct extensive experiments on five public RVOS benchmarks to demonstrate that our proposed ReferDINO outperforms state-of-the-art methods significantly. Project page: <https://isee-laboratory.github.io/ReferDINO>.

## 1. Introduction

Referring Video Object Segmentation (RVOS) [2, 35] aims to segment the target object in a video, referred by a given text description. This emerging task is potentially beneficial for many interactive video applications, and has therefore attracted great attention in the computer vision community. Compared to the unimodal video segmentation tasks [25, 36], RVOS is more challenging since it requires

\*Corresponding author.

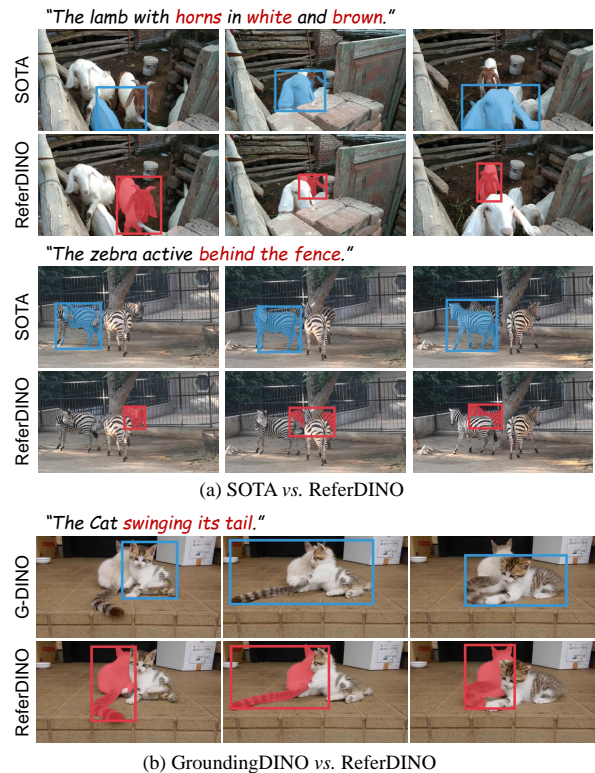


Figure 1. (a) The SOTA method [22] fails to handle the descriptions involving composite object attributes and spatial locations. (b) GroundingDINO [21] can neither understand the temporal dynamics nor perform pixel-wise segmentation.

a strong vision-language capability to understand complicated descriptions and associate visual objects with text.

Despite significant progress in recent years, existing RVOS models [2, 8, 22, 24, 35, 37] still suffer from many common problems. For example, they often struggle to handle the descriptions involving complicated object attributes and spatial locations, as shown in Figure 1 (a). These problems are mainly caused by the insufficient vision-language capabilities of current models, which, in turn, result from

the limited scale and diversity of available RVOS data.

In this work, we propose **ReferDINO**, an end-to-end RVOS approach that effectively addresses the above problems by inheriting strong vision-language understanding and spatial grounding capabilities from foundational visual grounding models. Represented by GroundingDINO [21], these foundation models benefit from extensive image-text pretraining and showcase strong potential in understanding complex object-text associations.

The critical challenges in adapting visual grounding models to the RVOS task are the lack of temporal understanding and pixel-wise segmentation capabilities, as illustrated in Figure 1 (b). To bridge these gaps and enable efficient adaptation to RVOS, we propose three key innovations in ReferDINO. First, we introduce an *object-consistent temporal enhancer* that leverages cross-modal text representations from foundational models to facilitate cross-frame object interaction, improving both temporal understanding and object consistency. Second, we elaborate a *grounding-guided deformable mask decoder*, which integrates both text and grounding conditions through efficient attention mechanisms to achieve accurate object segmentation. Third, we design a *confidence-aware query pruning strategy* to alleviate the computational bottlenecks without compromising performance, enabling our ReferDINO to satisfy the efficiency demands of video tasks.

These designs fully unleash the spatial grounding knowledge of pretrained foundation models and endow ReferDINO with effective temporal understanding and object segmentation capabilities. As shown in Figure 1, our ReferDINO overcomes the limitations of state-of-the-art RVOS models and the visual grounding models, enabling accurate referring video object segmentation.

Extensive experiments on five public RVOS benchmarks empirically show remarkable improvements of ReferDINO over state-of-the-art (SOTA) methods. For example, on Ref-DAVIS17 dataset, ReferDINO with the Swin-B backbone outperforms SOTAs by 4.0%  $\mathcal{J}\&\mathcal{F}$ . Moreover, compared to the competitive baseline [1] that combines GroundingDINO and SAM2 [27] for RVOS, ReferDINO demonstrates significant advantages in performance. For example, on Ref-Youtube-VOS dataset, ReferDINO with the Swin-T backbone improves the baseline by 12.0%  $\mathcal{J}\&\mathcal{F}$ . These results confirm the effectiveness of our designs over the foundation models. We summarize our contributions as follows:

- To the best of our knowledge, ReferDINO is the first end-to-end approach for adapting foundational visual grounding models to RVOS.
- We introduce three key innovations in ReferDINO to enable efficient object decoding, effective temporal understanding and accurate object segmentation.
- Our ReferDINO significantly outperforms SOTA methods across five public RVOS benchmarks.

## 2. Related Works

**Referring Video Object Segmentation.** RVOS [5, 6, 30] aims to segment objects throughout the video based on text descriptions. MTTR [2] firstly introduces the DETR paradigm [3] into RVOS. Furthermore, ReferFormer [35] proposes to produce the queries from the text description. On the top of this pipeline, follow-up works [7, 22, 24, 37] focus on modular improvements to improve cross-frame consistency and temporal understanding. Despite notable progress on specific datasets, these models are limited by insufficient vision-language understanding, and often struggle in unseen objects or scenarios. Recently, some works [1, 12] attempt to utilize GroundingDINO to identify objects in single frames and then apply independent segmentation models like SAM2 [27] to generate high-quality object masks. However, such a manner of model ensemble is inefficient and non-differentiable. Meanwhile, their performance almost completely relies on the static detection quality of GroundingDINO. In contrast, our ReferDINO is an end-to-end adaptation approach that benefits from both open-world knowledge of GroundingDINO and specific knowledge from RVOS data.

**Visual Grounding Foundation Model.** The aim of visual grounding [9, 11, 20, 29, 32, 33] is to locate the most relevant object or region in an image, based on a natural language query. Recent foundational works aim to unify detection datasets and image-text datasets through region-text matching, and exploit large image-text data to increase the training vocabulary at scale. GLIP [19] formulates object detection as a grounding problem, utilizing additional grounding data to promote hierarchical vision-language alignment. GroundingDINO [21] incorporates large-scale grounded pretraining into a strong object detector DINO [38] with deep cross-modality fusion. These models enable to capture object locations, attributions and variations based on natural language, and have been preliminary explored in some downstream tasks. For example, Video-GroundingDINO [34] enables GroundingDINO to predict event temporal boundaries by inserting a simple temporal self-attention module. Grounded-SAM [28] directly connects GroundingDINO with SAM [16] to achieve text-prompted image segmentation. In this work, we explore to adapt GroundingDINO for the RVOS task, and propose three critical innovations for efficient adaptation.

## 3. Background: GroundingDINO

Our approach builds on a visual grounding foundation model GroundingDINO [21], which we briefly revisit here. GroundingDINO is a DETR-architectural object detector, which introduces language to an object detector to achieve visual grounding. It mainly consists of an image backbone, a text backbone, a cross-modal encoder-decoder Trans-

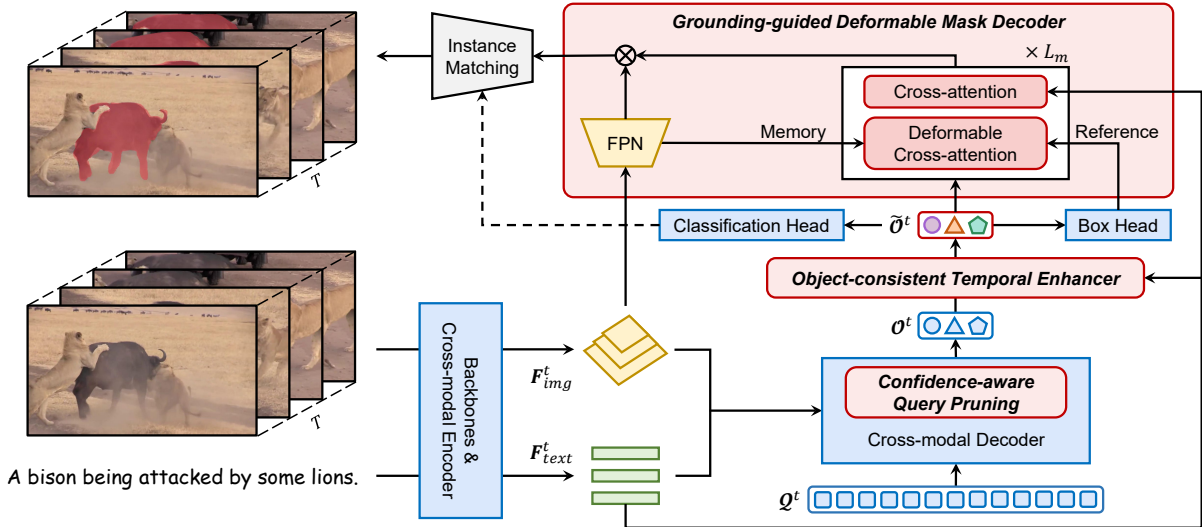


Figure 2. Overall architecture of ReferDINO. Modules colored in **blue** are borrowed from GroundingDINO, while those in **red** are newly introduced in this work. Based on the frame-wise object features  $\{\mathcal{O}^t\}_{t=1}^T$ , our *object-consistent temporal enhancer* leverages the cross-modal text features to enable inter-frame object interaction. Then, our *grounding-guided deformable mask decoder* produces masks for the candidate objects, conditioned on location predictions, cross-modal text features and high-resolution feature maps. To further improve the efficiency in video processing, we introduce a *confidence-aware query pruning* strategy in the cross-modal decoder. Best view in color.

former architecture, a box head and a classification head.

Given a pair of image and text, GroundingDINO adopts the dual backbones to extract vanilla features, and then input them into the cross-modal encoder to achieve enhanced image features  $F_{img}^t$  and text features  $F_{text}^t$ . These enhanced cross-modal features are used to initialize a large set of query embeddings, which are individually fed into a cross-modal decoder to generate object features. Finally, each object feature is passed to the box head and the classification head to predict the bounding boxes and scores. Here, the scores are defined as the similarities between an object feature and the text tokens. To adapt to RVOS, we define the binary probability of an object being referred to by the text as the maximum score of the object over all tokens.

## 4. ReferDINO

We illustrate our ReferDINO in Figure 2. Given a video clip of  $T$  frames and a text description, we employ GroundingDINO to derive the cross-modal image feature  $F_{img}^t$ , text feature  $F_{text}^t$  and object features  $\mathcal{O}^t$  of each individual frame. Then, we feed all the object features  $\{\mathcal{O}^t\}_{t=1}^T$  into *object-consistent temporal enhancer* (§4.1), which performs inter-frame object interactions and derives temporal enhanced object features  $\{\tilde{\mathcal{O}}^t\}_{t=1}^T$ . These features are passed through *grounding-guided deformable mask decoder* (§4.2) to produce instance masks, conditioned on the location predictions, cross-modal text features and high-resolution feature maps. To improve the efficiency with-

out compromising performance, we introduce a *confidence-aware query pruning* strategy (§4.3) in the cross-modal decoder. We detail the training and inference in §4.4.

### 4.1. Object-consistent Temporal Enhancer

Although GroundingDINO can detect referring objects from single images, this is not reliable enough for RVOS. First, it lacks the capability to capture temporal dynamics in videos, making it unable to handle motion-related descriptions, e.g., “the cat swing its tail”. Second, video frames often contain camera motion blur and constrained perspectives, which greatly undermine the temporal consistency of GroundingDINO. To overcome these limitations, we propose *object-consistent temporal enhancer* upon the GroundingDINO. This module performs inter-frame object interactions under the text guidance, enabling our ReferDINO to capture effective temporal associations between visual objects and text descriptions.

As shown in Figure 3, the proposed object-consistent temporal enhancer consist of a memory-augmented tracker and a cross-modal temporal decoder. It receives two inputs: all the object embeddings  $\{\mathcal{O}^t\}_{t=1}^T$ , and all the cross-modal sentence features  $\{f_{cls}^t\}_{t=1}^T$ , where  $f_{cls}^t$  corresponds to the [CLS] token in the text feature  $F_{text}^t$ .

**Memory-augmented Tracker.** Before temporal interaction, we need to align the objects across different frames with a tracker module. Different from the trackers used in previous works [5, 8] that only consider the alignment between adjacent frames, we integrate a memory mechanism

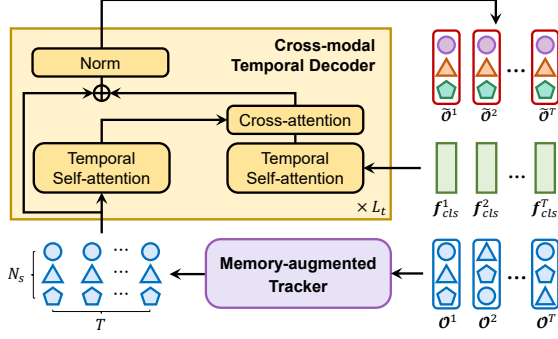


Figure 3. Illustration of our *object-consistent temporal enhancer*, where  $f_{cls}^t$  is the cross-modal sentence feature of  $t$ -th frame.

for stable long-term tracking. Let  $\mathcal{M}^t$  indicates the memory for  $t$ -th frame, and  $\mathcal{M}^1 = \mathcal{O}^1$ . Our memory-augmented tracker consist of two steps: *object alignment* and *memory updating*. In the first step, we compute the cosine similarity between  $\mathcal{M}^{t-1}$  and  $\mathcal{O}^t$  as the assignment cost, and apply the Hungarian algorithm [17] to align the objects with the memory:

$$\hat{\mathcal{O}}^t = \text{Hungarian}(\mathcal{M}^{t-1}, \mathcal{O}^t), \quad (1)$$

where  $\hat{\mathcal{O}}^t$  indicates the aligned object embeddings. In the second step, these embeddings are used to update the memory in a momentum-based manner. Meanwhile, we incorporate the text relevance to adaptively prevent object-invisible frames from disturbing the long-term memory. Formally, the memory is updated as follows:

$$\mathcal{M}^t = (1 - \alpha \cdot c^t) \cdot \mathcal{M}^{t-1} + \alpha \cdot c^t \cdot \hat{\mathcal{O}}^t, \quad (2)$$

where  $\alpha$  is the momentum coefficient, and  $c \in \mathbb{R}^{N_s}$  is the cosine similarity between  $\hat{\mathcal{O}}^t \in \mathbb{R}^{N_s \times d}$  and its sentence embedding  $f_{cls}^t \in \mathbb{R}^d$ .

**Cross-modal Temporal Dehancer.** This module takes the frame-wise sentence embeddings as frame proxies to perform inter-frame interaction and video-level object enhancement. Specifically, this module comprises  $L_t$  blocks. In each block, given the aligned object embeddings  $\{\hat{\mathcal{O}}^t\}_{t=1}^T$  and the sentence embeddings  $\{f_{cls}^t\}_{t=1}^T$ , we employ self-attention along the temporal dimension to achieve inter-frame interaction. Next, we extract video-level object information with a cross-attention module, which takes the sentence embeddings as *query* and the object embeddings as *key* and *value*, deriving video-level object representations  $\{\mathcal{O}_v^t\}_{t=1}^T$ . These representations, containing effective temporal information, are used to enhance the frame-wise object embeddings as follows:

$$\tilde{\mathcal{O}}^t = \text{LayerNorm}(\hat{\mathcal{O}}^t + \mathcal{O}_v^t). \quad (3)$$

## 4.2. Grounding-guided Deformable Mask Decoder

To fully leverage GroundingDINO’s pretrained capabilities for object segmentation, we customize a novel *grounding-guided deformable mask decoder*. This decoder integrates the pretrained representations and grounding predictions from GroundingDINO to iteratively refine the mask embeddings, enabling accurate and consistent object segmentation throughout the video.

For simplicity, we use  $\tilde{o}$  to represent an arbitrary object in  $\tilde{\mathcal{O}}^t$ . Before the mask decoder, we feed  $\tilde{o}$  into the bounding box to predict its bounding box  $\mathbf{b} \in \mathbb{R}^4$ , where  $\mathbf{b} = \{b_x, b_y, b_w, b_h\}$  encodes the normalized box center coordinates, box height and width. Meanwhile, we employ a feature pyramid network (FPN) upon the cross-modal image features  $F_{\text{img}}$ , producing a high-resolution feature map  $F_{\text{seg}} \in \mathbb{R}^{\frac{H}{4} \times \frac{W}{4} \times d}$ , where  $H$  and  $W$  denote the height and width of the raw video frames.

Then, we input these features and box predictions into the *grounding-guided deformable mask decoder* for object refinement and mask generation. This mask decoder consists of  $L_m$  blocks, with each block comprising two components: deformable cross-attention [39] and vanilla cross-attention. The deformable cross-attention integrates the pretrained grounding knowledge by taking  $\tilde{o}$  as *query*,  $F_{\text{seg}}$  as *memory* and the box center  $\{b_x, b_y\}$  as *reference point*. This mechanism efficiently aggregates the spatial information around predicted locations for object refinement. The vanilla cross-attention is used to integrate the text conditions, by taking  $\tilde{o}$  as *query* and  $F_{\text{text}}$  as *key* and *value*. These two components work together to ensure that object segmentation is tightly coupled with both the text prompts and visual grounding. Finally, for each object query, we obtain a refined mask embedding  $o_m \in \mathbb{R}^d$ , which is then dot-producted with the high-resolution feature map  $F_{\text{seg}}$  to generate an instance mask  $\mathbf{m}$ .

## 4.3. Confidence-aware Query Pruning

Foundational visual grounding models typically utilize a large set of query embeddings to store extensive object information, e.g., GroundingDINO uses  $N_q = 900$  queries in the cross-modal decoder. Iteratively processing such a large amount of queries significantly limits the efficiency, especially in video processing. However, directly reducing these queries can compromise the well-pretrained object knowledge. To solve this dilemma, we propose a *confidence-aware query pruning* strategy to iteratively reject the low-confidence queries at each decoder layer, deriving only a compact set of important queries for subsequent computations, as shown in Figure 4.

Specifically, the cross-modal decoder is stacked by 6 layers, and each layer consists of a self-attention, a cross-attention with image features and a cross-attention with text features. Let  $Q_l \in \mathbb{R}^{N_l \times d}$  denote the output query embed-

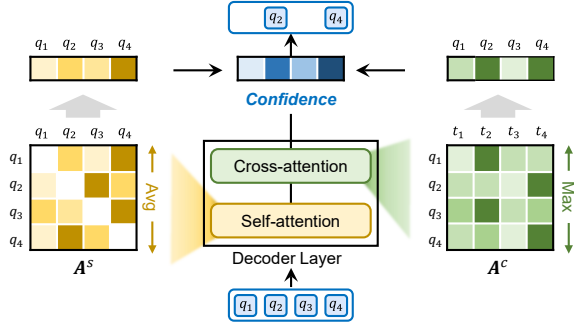


Figure 4. Illustration of our *confidence-aware query pruning*, where  $q_i$  and  $t_i$  indicate  $i$ -th query and text token, respectively.

dings of the  $l$ -th decoder layer, where  $N_0 = N_q$ . We reuse the attention weights in the decoder layer to compute a confidence score for each query as follows:

$$s_j = \frac{1}{N_l - 1} \sum_{i=1, i \neq j}^{N_l} \mathbf{A}_{ij}^s + \max_k \mathbf{A}_{kj}^c, \quad (4)$$

where  $s_j$  is the confidence of  $j$ -th query,  $\mathbf{A}^s \in \mathbb{R}^{N_l \times N_l}$  denotes the self-attention weight,  $\mathbf{A}^c \in \mathbb{R}^{L \times N_l}$  denotes the transposed cross-attention weight with  $L$  text tokens. The former term represents the average attention received by  $j$ -th query from other queries. A query receiving high attention from others typically indicates that it is irreplaceable. The latter maximum term measures the probability that  $j$ -th query (i.e., object) is mentioned in the text. The combination of these two terms represents the query importance and the relevance to text descriptions. Based on this score, we filter out  $p\%$  of the low-confidence object queries at each layer, finally yielding a compact set of  $N_s$  object embeddings, where  $N_s \ll N_q$ . This strategy significantly reduces the computation costs without compromising performance, enabling our ReferDINO to satisfy the efficiency demands of video processing.

#### 4.4. Training and Inference

ReferDINO ultimately produces  $N_s$  object prediction sequences  $\mathbf{p} = \{\mathbf{p}_i\}_{i=1}^{N_s}$  for a video-text pair, and each sequence is represented by  $\mathbf{p}_i = \{\mathbf{c}_i^t, \mathbf{b}_i^t, \mathbf{m}_i^t\}_{t=1}^T$ , which denotes the binary classification probability, bounding box and mask of the  $i$ -th object query on  $t$ -th frame. Note that there is only one object sequence correctly corresponding to the text description.

**Training.** Suppose the ground truth object sequence to be  $\mathbf{y} = \{\mathbf{c}^t, \mathbf{b}^t, \mathbf{m}^t\}_{t=1}^T$ . During training, we select the sequence with the lowest matching cost as the positive and assign the remaining sequences as negative. The matching

cost is defined as follows:

$$\mathcal{L}_{\text{total}}(\mathbf{y}, \mathbf{p}_i) = \lambda_{\text{cls}} \mathcal{L}_{\text{cls}}(\mathbf{y}, \mathbf{p}_i) + \lambda_{\text{box}} \mathcal{L}_{\text{box}}(\mathbf{y}, \mathbf{p}_i) + \lambda_{\text{mask}} \mathcal{L}_{\text{mask}}(\mathbf{y}, \mathbf{p}_i). \quad (5)$$

The matching cost is computed on individual frames and normalized by the frame number. Here,  $\mathcal{L}_{\text{cls}}$  is the focal loss that supervises the binary classification prediction.  $\mathcal{L}_{\text{box}}$  sums up the L1 loss and GIoU loss.  $\mathcal{L}_{\text{mask}}$  is the combination of DICE loss, binary mask focal loss and projection loss [31].  $\lambda_{\text{cls}}$ ,  $\lambda_{\text{box}}$  and  $\lambda_{\text{mask}}$  are scalar weights of individual losses. The model is optimized end-to-end by minimizing the total loss  $\mathcal{L}_{\text{total}}$  for positive sequences and only the classification loss  $\mathcal{L}_{\text{cls}}$  for negative sequences.

**Inference.** At inference, we select the best sequence with the highest average classification score, and its index is denoted as follows:

$$\sigma = \arg \max_{i \in [1, N_s]} \frac{\sum_{t=1}^T \mathbf{c}_i^t}{T}. \quad (6)$$

Finally, the output mask sequence is formed as  $\{\mathbf{m}_\sigma^t\}_{t=1}^T$ .

## 5. Experiments

### 5.1. Experimental Setup

**Datasets.** We evaluate ReferDINO on five public benchmarks: Ref-YouTube-VOS [30], Ref-DAVIS17 [15], A2D-Sentences, JHMDB-Sentences [6] and MeViS [5]. Ref-YouTube-VOS is a large-scale dataset covering 3,978 videos with 15K text descriptions. Ref-DAVIS17, A2D-Sentences and JHMDB-Sentences are created by annotating additional text descriptions on the original DAVIS17 [26], A2D [13] and JHMDB datasets, respectively. Ref-DAVIS17 contains 90 videos and 1.5K text descriptions. A2D-Sentences consists of 3.7K videos and 6.6K text descriptions. JHMDB-Sentences provides 928 videos, each with a description. MeViS is a recently established benchmark that poses new challenges in cross-modal motion understanding, including 2K videos and 28K text descriptions.

**Metrics.** Following previous works, we use region similarity  $\mathcal{J}$  (average IoU), contour accuracy  $\mathcal{F}$  (mean boundary similarity), and their average  $\mathcal{J}\&\mathcal{F}$  on MeViS, Ref-YouTube-VOS and Ref-DAVIS17. For A2D-Sentences and JHMDB-Sentences, we employ mAP, overall IoU (oIoU), and mean IoU (mIoU) metrics. All evaluations are conducted using the official code or online platforms.

**Protocols.** We follow the experimental protocols established in previous works. Specifically, the model trained on the training set of Ref-YouTube-VOS is directly evaluated on the validation splits of Ref-YouTube-VOS and Ref-DAVIS17. Similarly, the model trained on A2D-Sentences is directly evaluated on A2D-Sentences and

Method	Venue	Ref-YouTube-VOS			Ref-DAVIS17			A2D-Sentences			JHMDB-Sentences		
		$\mathcal{J}\&\mathcal{F}$	$\mathcal{J}$	$\mathcal{F}$	$\mathcal{J}\&\mathcal{F}$	$\mathcal{J}$	$\mathcal{F}$	mAP	oIoU	mIoU	mAP	oIoU	mIoU
<i>Video-Swin-T / Swin-T</i>													
ReferFormer [35]	CVPR'22	59.4	58.0	60.9	59.6	56.5	62.7	52.8	77.6	69.6	42.2	71.9	71.0
HTML [7]	ICCV'23	61.2	59.5	63.0	-	-	-	53.4	77.6	69.2	42.7	-	-
SgMg [24]	ICCV'23	62.0	60.4	63.5	61.9	59.0	64.8	56.1	78.0	70.4	44.4	72.8	71.7
SOC [22]	NIPS'23	62.4	61.1	63.7	63.5	60.2	66.7	54.8	78.3	70.6	42.7	72.7	71.6
LoSh [37]	CVPR'24	63.7	62.0	65.4	62.9	60.1	65.7	57.6	79.3	71.6	-	-	-
DsHmp [8]	CVPR'24	63.6	61.8	65.4	64.0	60.8	67.2	57.2	79.0	71.3	44.9	73.1	72.1
Grounded-SAM2 [1]	arXiv'24	54.4	51.8	57.0	60.9	57.4	62.6	47.5	59.0	62.5	38.9	70.8	70.5
<b>ReferDINO (ours)</b>	-	<b>66.4</b>	<b>64.4</b>	<b>68.4</b>	<b>66.8</b>	<b>63.1</b>	<b>70.5</b>	<b>58.9</b>	<b>80.2</b>	<b>72.3</b>	<b>45.6</b>	<b>74.2</b>	<b>73.1</b>
<i>Video-Swin-B / Swin-B</i>													
ReferFormer [35]	CVPR'22	62.9	61.3	64.6	61.1	58.1	64.1	55.0	78.6	70.3	43.7	73.0	71.8
HTML [7]	ICCV'23	63.4	61.5	65.2	62.1	59.2	65.1	56.7	79.5	71.2	44.2	-	-
SgMg [24]	ICCV'23	65.7	63.9	67.4	63.3	60.6	66.0	58.5	79.9	72.0	45.0	73.7	72.5
SOC [22]	NIPS'23	66.0	64.1	67.9	64.2	61.0	67.4	57.3	80.7	72.5	44.6	73.6	72.3
LoSh [37]	CVPR'24	67.2	65.4	69.0	64.3	61.8	66.8	59.9	81.2	73.1	-	-	-
DsHmp [8]	CVPR'24	67.1	65.0	69.1	64.9	61.7	68.1	59.8	81.1	72.9	45.8	73.9	73.0
Grounded-SAM2 [1]†	arXiv'24	64.8	62.5	67.0	66.2	62.6	69.7	54.7	67.8	68.5	42.5	72.1	72.1
<b>ReferDINO (ours)</b>	-	<b>69.3</b>	<b>67.0</b>	<b>71.5</b>	<b>68.9</b>	<b>65.1</b>	<b>72.9</b>	<b>61.1</b>	<b>82.1</b>	<b>73.6</b>	<b>46.6</b>	<b>74.2</b>	<b>73.2</b>

Table 1. Comparison on Ref-YouTube-VOS, Ref-DAVIS17, A2D-Sentences and JHMDB-Sentences. †The results are obtained from [12].

JHMDB-Sentences. The model is first pretrained on referring image segmentation datasets RefCOCO+/-g [14, 23], and then trained on the RVOS datasets, except for MeViS where the model is trained directly, following [5, 8].

**Implementation Details.** Our model is built upon the pre-trained GroundingDINO, which uses Swin Transformer as the image backbone and BERT as the text backbone. The official source releases two GroundingDINO checkpoints: Swin-T and Swin-B, both of which are covered in our experiments. We freeze the GroundingDINO’s backbones and finetune the cross-modal Transformer with LoRA techniques [10], where the rank is set to 32. We set  $\alpha = 0.1$ ,  $L_t = 3$ , and  $L_m = 3$ . In the query pruning, we set the drop rate as 50%. For MeViS dataset involving multiple target objects, we follow the practice in [5, 8] to select multiple object trajectories with classification scores higher than a threshold  $\sigma = 0.2$ . For the other datasets, we select the best object trajectory by Equation 6.

## 5.2. Main Results

**Comparisons with SOTA Methods.** As shown in Tables 1 and 2, our ReferDINO significantly and consistently outperforms SOTA methods across all five RVOS datasets. Specifically, with the Swin-T backbone, our ReferDINO achieves 48.0%  $\mathcal{J}\&\mathcal{F}$  on the challenging dataset MeViS, outperforming existing SOTA by 1.6%. On the competitive dataset Ref-YouTube-VOS, our ReferDINO achieves 66.4%  $\mathcal{J}\&\mathcal{F}$ , improving SOTA performance by 2.8%. When a larger backbone Swin-B is applied, ReferDINO further improves  $\mathcal{J}\&\mathcal{F}$  to 69.3% on Ref-YouTube-VOS, surpassing SOTA by more than 2.2%. Consistent performance improvements are observed across the other datasets, which demonstrates the superiority of our ReferDINO model.

Method	Venue	$\mathcal{J}\&\mathcal{F}$	$\mathcal{J}$	$\mathcal{F}$
<i>Video-Swin-T / Swin-T</i>				
MTTR [2]	CVPR'22	30.0	28.8	31.2
ReferFormer [35]	CVPR'22	31.0	29.8	32.2
LMPM [5]	ICCV'23	37.2	34.2	40.2
DsHmp [8]	CVPR'24	46.4	43.0	49.8
Grounded-SAM2 [1]	arXiv'24	37.4	31.0	43.7
<b>ReferDINO (ours)</b>	-	<b>48.0</b>	<b>43.6</b>	<b>52.3</b>
<i>Video-Swin-B / Swin-B</i>				
Grounded-SAM2 [1]	arXiv'24	40.5	34.5	46.4
<b>ReferDINO (ours)</b>	-	<b>49.3</b>	<b>44.7</b>	<b>53.9</b>

Table 2. Comparison on MeViS.

**Comparisons with GroundingDINO+SAM2.** To demonstrate the effectiveness of our module designs upon GroundingDINO, we compare against a recent baseline Grounded-SAM2 [1], which uses GroundingDINO to identify objects in a single frame and then feed the box outputs into SAM2 [27] for segmenting throughout the video. We run with the official code and adopt the `sam2_hiera_large` version of SAM2. As shown in Tables 1 and 2, the performance of Grounded-SAM2 heavily depends on the detection quality of GroundingDINO. For example, switching GroundingDINO from Swin-B to Swin-T results in a drastic 10.4% drop in  $\mathcal{J}\&\mathcal{F}$  on Ref-YouTube-VOS. Besides, such simple model ensemble cannot effectively address the RVOS task. Across various datasets and backbones, our ReferDINO consistently outperforms Grounded-SAM2 by a significant margin. This demonstrates the effectiveness of our approach in adapting GroundingDINO to RVOS task.

## 5.3. Ablation Studies

Our model is built upon GroundingDINO with three elaborated designs, which we ablate in this section. We use MeViS as the main dataset as it is the largest.

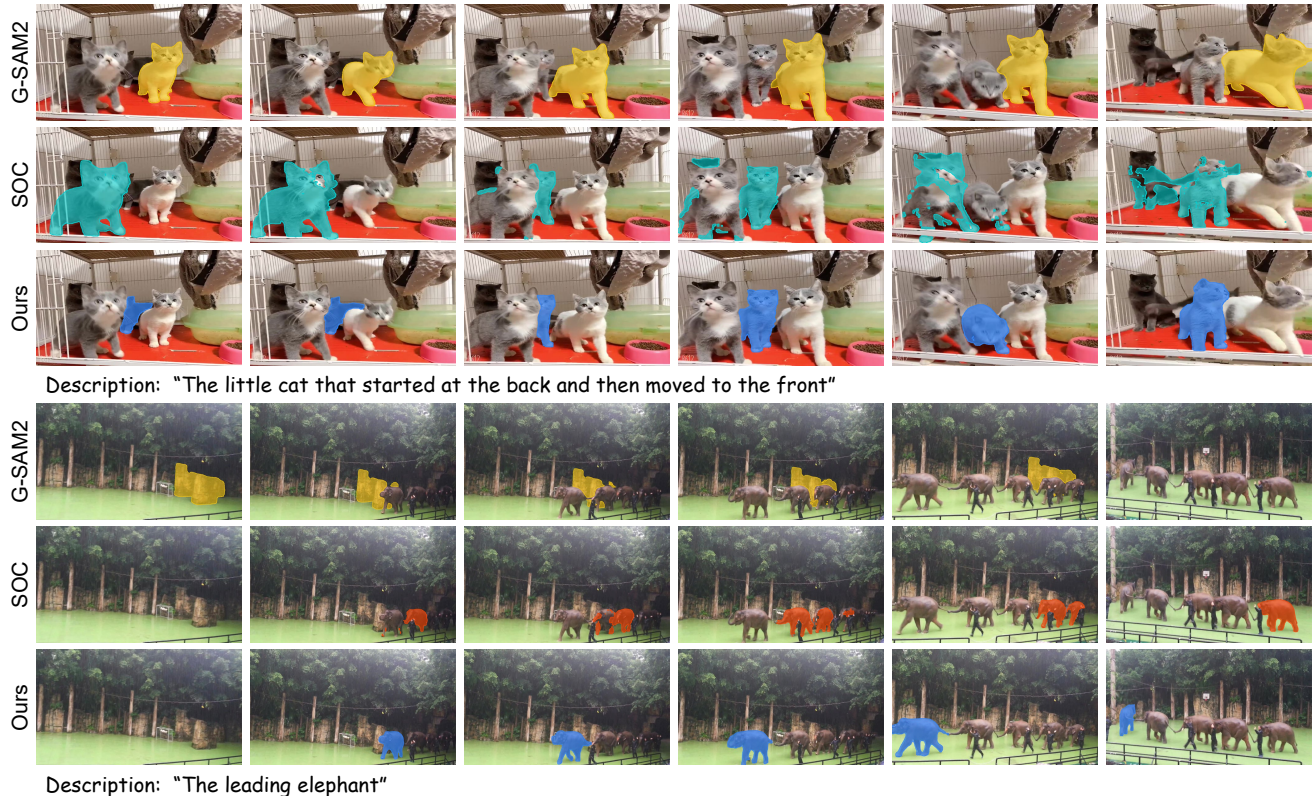


Figure 5. Qualitative comparison of our ReferDINO with others.

Method	$\mathcal{J}\&\mathcal{F}$	$\mathcal{J}$	$\mathcal{F}$
<b>Ours</b>	<b>48.0</b>	<b>43.6</b>	<b>52.3</b>
w/o Tracker	47.6	43.2	52.1
w/o Decoder	45.8	42.7	48.8

Table 3. Ablation study of the temporal aggregator.

Mask Decoder	$\mathcal{J}\&\mathcal{F}$	$\mathcal{J}$	$\mathcal{F}$
Dot-product	45.0	41.4	48.5
CondInst [31]	44.4	40.7	48.1
<b>Ours</b>	<b>48.0</b>	<b>43.6</b>	<b>52.3</b>
w/o CA	47.6	43.1	52.0
w/o DCA	45.3	41.8	48.7

Table 4. Ablation study of the mask decoder.

**Temporal Enhancer.** Our *object-consistent temporal enhancer* consists of a memory-augmented tracker and a cross-modal temporal decoder. We analyze their individual contributions in Table 3. First, while the object queries in GroundingDINO is naturally aligned across frames to some extent, adding a tracker can still improve the temporal consistency, leading to a 0.4% improvement in  $\mathcal{J}\&\mathcal{F}$ . Second, in the temporal decoder is essential for understanding temporal dynamics and object motion, providing 2.2% improvements in  $\mathcal{J}\&\mathcal{F}$ . These results demonstrates the effectiveness of our object-consistent temporal enhancer.

**Mask Decoder.** We evaluate the effectiveness of our proposed *grounding-guided deformable mask decoder* by re-

placing it with two widely used mask decoders: *dot-product head* directly dot products each object query embedding with the feature map to produce pixel-wise probabilities, while *CondInst* [31] utilizes each query embedding to generate kernels and then performs convolution on the feature map. The former has been adopted in many DETR-based segmentation models [4, 8, 18] and the latter is widely used in previous RVOS works [22, 35, 37]. As shown in Table 4, our mask decoder outperforms the dot-product head and CondInst by 3.0% and 3.6%  $\mathcal{J}\&\mathcal{F}$ , respectively. This demonstrates the importance of integrating pretrained grounding knowledge to guide segmentation. We also ablate the cross-attention (CA) and deformable cross-attention (DCA) in the mask decoder to validate the effectiveness of our module designs. As shown at the bottom of Table 4, removing CA and DCA results in performance drops of 0.4% and 2.7% in  $\mathcal{J}\&\mathcal{F}$ , respectively. These results demonstrate the effectiveness of our modular design.

**Query Pruning.** We explore the effects of different drop rates. Since training with more than 50% of queries on MeViS is highly time-consuming, we perform this validation on the Ref-YouTube-VOS dataset, and present the training costs and test results in Table 5. It shows that our confidence-aware query pruning can maintain the performance while significantly reducing the computational costs.



Figure 6. Visualization of our ReferDINO for multiple text references.

Drop Rate	$\mathcal{J}\&\mathcal{F}$	$\mathcal{J}$	$\mathcal{F}$	FLOPs	Memory
0	66.3	64.2	68.3	1352G	26.8G
20%	66.5	64.5	68.5	1068G	20.4G
50%	66.4	64.4	68.4	896G	17.0G
65%	66.0	64.0	68.0	857G	16.2G
Random 50%	41.1	39.2	42.9	896G	16.9G

Table 5. Ablation study of query pruning on Ref-YouTube-VOS. FLOPs and Memory are measured under batch size of 1, video shape of [6, 3, 368, 640] and with Pytorch checkpointing disabled.

For instance, reducing 50% queries with our strategy gains 0.1% in  $\mathcal{J}\&\mathcal{F}$ , while dramatically decreasing FLOPs and Memory by 33.7% and 36.6%, respectively. In contrast, randomly dropping the same number of queries results in a substantial 25.2% decrease in  $\mathcal{J}\&\mathcal{F}$ . By employing this query pruning strategy, we can efficiently train ReferDINO on large RVOS datasets without compromising the pre-trained knowledge within GroundingDINO’s queries. To balance efficiency and performance, we set the drop rate to 50% by default.

#### 5.4. Qualitative Analysis

**Qualitative Comparison.** In Figure 5, we compare the qualitative results of our ReferDINO with Grounded-SAM2 [1] and SOC [22]. Powered by SAM2 [27], Grounded-SAM2 can produce high-quality masks. However, it lacks the ability to understand temporal dynamics and motion, often resulting in misidentification of referred objects. SOC performs better at identification, but its segmentation quality and temporal consistency are less effective. By contrast, our ReferDINO effectively addresses both challenges, enabling accurate referred object identification,

“The little cat that started at the back and then moved to the front.”

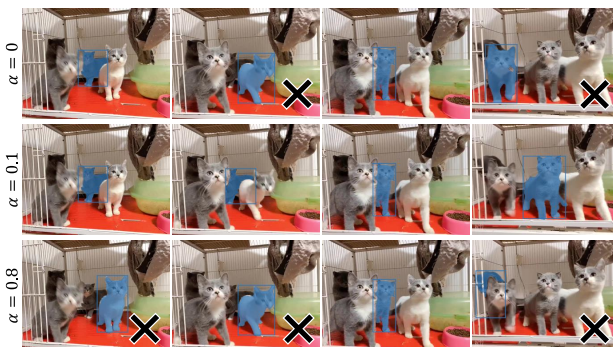


Figure 7. Qualitative impacts of  $\alpha$  in memory-augmented tracker. We use  $\times$  to highlight the incorrect results.

stable object tracking and high-quality object segmentation.

**Visualization of Multiple References.** In Figure 6, we present several visualizations of our ReferDINO processing various text references within a video. These results clearly demonstrate the effectiveness of ReferDINO in motion comprehension, spatio-temporal reasoning and vision-language understanding.

**Visualization of Object Consistency.** The momentum coefficient  $\alpha$  controls the amplitude of memory updating. We visualize a case in Figure 7 to show its impact on temporal consistency. In this case, a smaller  $\alpha$  yields the best performance. This is because the identification in the initial frames is crucial for capturing the clue “started at the back”. In our main experiments, we set  $\alpha = 0.1$  by default.



## 6. Conclusion

In this work, we propose ReferDINO, a strong and robust end-to-end RVOS model. ReferDINO is built upon the foundational visual grounding model GroundingDINO, with three significant innovations. First, we introduce a grounding-guided deformable mask decoder, which integrates the pretrained capabilities of GroundingDINO to generate accurate object masks. Second, we design an object-consistent temporal enhancer to enhance temporal understanding and tracking consistency. Third, we propose a confidence-aware query pruning strategy, which significantly accelerates the object decoding process without compromising performance. Extensive experiments across five public benchmarks demonstrate that ReferDINO significantly outperforms existing RVOS methods.

## References

- [1] Grounded-SAM-2. <https://github.com/IDEA-Research/Grounded-SAM-2>. 2, 6, 8
- [2] Adam Botach, Evgenii Zheltonozhskii, and Chaim Baskin. End-to-end referring video object segmentation with multi-modal transformers. In *Proceedings of the IEEE/CVF Conference on Computer Vision and Pattern Recognition*, pages 4985–4995, 2022. 1, 2, 6
- [3] Nicolas Carion, Francisco Massa, Gabriel Synnaeve, Nicolas Usunier, Alexander Kirillov, and Sergey Zagoruyko. End-to-end object detection with transformers. In *European conference on computer vision*, pages 213–229. Springer, 2020. 2
- [4] Wuyang Chen, Xianzhi Du, Fan Yang, Lucas Beyer, Xiaohua Zhai, Tsung-Yi Lin, Huizhong Chen, Jing Li, Xiaodan Song, Zhangyang Wang, et al. A simple single-scale vision transformer for object localization and instance segmentation. *arXiv preprint arXiv:2112.09747*, 2021. 7
- [5] Henghui Ding, Chang Liu, Shuting He, Xudong Jiang, and Chen Change Loy. Mevis: A large-scale benchmark for video segmentation with motion expressions. In *Proceedings of the IEEE/CVF International Conference on Computer Vision*, pages 2694–2703, 2023. 2, 3, 5, 6
- [6] Kirill Gavriluk, Amir Ghodrati, Zhenyang Li, and Cees GM Snoek. Actor and action video segmentation from a sentence. In *Proceedings of the IEEE conference on computer vision and pattern recognition*, pages 5958–5966, 2018. 2, 5
- [7] Mingfei Han, Yali Wang, Zhihui Li, Lina Yao, Xiaojuan Chang, and Yu Qiao. Htm1: Hybrid temporal-scale multimodal learning framework for referring video object segmentation. In *Proceedings of the IEEE/CVF International Conference on Computer Vision*, pages 13414–13423, 2023. 2, 6
- [8] Shuting He and Henghui Ding. Decoupling static and hierarchical motion perception for referring video segmentation. In *Proceedings of the IEEE/CVF Conference on Computer Vision and Pattern Recognition*, pages 13332–13341, 2024. 1, 3, 6, 7
- [9] Richang Hong, Daqing Liu, Xiaoyu Mo, Xiangnan He, and Hanwang Zhang. Learning to compose and reason with language tree structures for visual grounding. *IEEE transactions on pattern analysis and machine intelligence*, 44(2): 684–696, 2019. 2
- [10] Edward J Hu, Yelong Shen, Phillip Wallis, Zeyuan Allen-Zhu, Yuanzhi Li, Shean Wang, Lu Wang, and Weizhu Chen. Lora: Low-rank adaptation of large language models. *arXiv preprint arXiv:2106.09685*, 2021. 6
- [11] Ronghang Hu, Marcus Rohrbach, Jacob Andreas, Trevor Darrell, and Kate Saenko. Modeling relationships in referential expressions with compositional modular networks. In *Proceedings of the IEEE conference on computer vision and pattern recognition*, pages 1115–1124, 2017. 2
- [12] Shaofei Huang, Rui Ling, Hongyu Li, Tianrui Hui, Zongheng Tang, Xiaoming Wei, Jizhong Han, and Si Liu. Unleashing the temporal-spatial reasoning capacity of gpt for training-free audio and language referenced video object segmentation. *arXiv preprint arXiv:2408.15876*, 2024. 2, 6
- [13] Hueihan Jhuang, Juergen Gall, Silvia Zuffi, Cordelia Schmid, and Michael J Black. Towards understanding action recognition. In *Proceedings of the IEEE international conference on computer vision*, pages 3192–3199, 2013. 5
- [14] Sahar Kazemzadeh, Vicente Ordonez, Mark Matten, and Tamara Berg. Referitgame: Referring to objects in photographs of natural scenes. In *Proceedings of the 2014 conference on empirical methods in natural language processing (EMNLP)*, pages 787–798, 2014. 6
- [15] Anna Khoreva, Anna Rohrbach, and Bernt Schiele. Video object segmentation with language referring expressions. In *Computer Vision—ACCV 2018: 14th Asian Conference on Computer Vision, Perth, Australia, December 2–6, 2018, Revised Selected Papers, Part IV 14*, pages 123–141. Springer, 2019. 5
- [16] Alexander Kirillov, Eric Mintun, Nikhila Ravi, Hanzi Mao, Chloe Rolland, Laura Gustafson, Tete Xiao, Spencer Whitehead, Alexander C Berg, Wan-Yen Lo, et al. Segment anything. In *Proceedings of the IEEE/CVF International Conference on Computer Vision*, pages 4015–4026, 2023. 2
- [17] Harold W Kuhn. The hungarian method for the assignment problem. *Naval research logistics quarterly*, 2(1-2):83–97, 1955. 4
- [18] Feng Li, Hao Zhang, Huaizhe Xu, Shilong Liu, Lei Zhang, Lionel M Ni, and Heung-Yeung Shum. Mask dino: Towards a unified transformer-based framework for object detection and segmentation. In *Proceedings of the IEEE/CVF Conference on Computer Vision and Pattern Recognition*, pages 3041–3050, 2023. 7
- [19] Liunian Harold Li, Pengchuan Zhang, Haotian Zhang, Jianwei Yang, Chunyuan Li, Yiwu Zhong, Lijuan Wang, Lu Yuan, Lei Zhang, Jenq-Neng Hwang, et al. Grounded language-image pre-training. In *Proceedings of the IEEE/CVF Conference on Computer Vision and Pattern Recognition*, pages 10965–10975, 2022. 2
- [20] Yue Liao, Si Liu, Guanbin Li, Fei Wang, Yanjie Chen, Chen Qian, and Bo Li. A real-time cross-modality correlation filtering method for referring expression comprehension. In *Proceedings of the IEEE/CVF Conference on Computer Vision and Pattern Recognition*, pages 10880–10889, 2020. 2

- [21] Shilong Liu, Zhaoyang Zeng, Tianhe Ren, Feng Li, Hao Zhang, Jie Yang, Chunyuan Li, Jianwei Yang, Hang Su, Jun Zhu, et al. Grounding dino: Marrying dino with grounded pre-training for open-set object detection. In *European Conference on Computer Vision*, 2024. 1, 2
- [22] Zhuoyan Luo, Yicheng Xiao, Yong Liu, Shuyan Li, Yitong Wang, Yansong Tang, Xiu Li, and Yujiu Yang. Soc: semantic-assisted object cluster for referring video object segmentation. In *Proceedings of the 37th International Conference on Neural Information Processing Systems*, pages 26425–26437, 2023. 1, 2, 6, 7, 8
- [23] Junhua Mao, Jonathan Huang, Alexander Toshev, Oana Camburu, Alan L Yuille, and Kevin Murphy. Generation and comprehension of unambiguous object descriptions. In *Proceedings of the IEEE conference on computer vision and pattern recognition*, pages 11–20, 2016. 6
- [24] Bo Miao, Mohammed Bennamoun, Yongsheng Gao, and Ajmal Mian. Spectrum-guided multi-granularity referring video object segmentation. In *Proceedings of the IEEE/CVF International Conference on Computer Vision*, pages 920–930, 2023. 1, 2, 6
- [25] Federico Perazzi, Jordi Pont-Tuset, Brian McWilliams, Luc Van Gool, Markus Gross, and Alexander Sorkine-Hornung. A benchmark dataset and evaluation methodology for video object segmentation. In *Proceedings of the IEEE conference on computer vision and pattern recognition*, pages 724–732, 2016. 1
- [26] Jordi Pont-Tuset, Federico Perazzi, Sergi Caelles, Pablo Arbeláez, Alex Sorkine-Hornung, and Luc Van Gool. The 2017 davis challenge on video object segmentation. *arXiv preprint arXiv:1704.00675*, 2017. 5
- [27] Nikhila Ravi, Valentin Gabeur, Yuan-Ting Hu, Ronghang Hu, Chaitanya Ryali, Tengyu Ma, Haitham Khedr, Roman Rädle, Chloe Rolland, Laura Gustafson, Eric Mintun, Junting Pan, Kalyan Vasudev Alwala, Nicolas Carion, Chaoyuan Wu, Ross Girshick, Piotr Dollár, and Christoph Feichtenhofer. Sam 2: Segment anything in images and videos. *arXiv preprint arXiv:2408.00714*, 2024. 2, 6, 8
- [28] Tianhe Ren, Shilong Liu, Ailing Zeng, Jing Lin, Kunchang Li, He Cao, Jiayu Chen, Xinyu Huang, Yukang Chen, Feng Yan, et al. Grounded sam: Assembling open-world models for diverse visual tasks. *arXiv preprint arXiv:2401.14159*, 2024. 2
- [29] Arka Sadhu, Kan Chen, and Ram Nevatia. Zero-shot grounding of objects from natural language queries. In *Proceedings of the IEEE/CVF International Conference on Computer Vision*, pages 4694–4703, 2019. 2
- [30] Seonguk Seo, Joon-Young Lee, and Bohyung Han. Urvos: Unified referring video object segmentation network with a large-scale benchmark. In *Computer Vision—ECCV 2020: 16th European Conference, Glasgow, UK, August 23–28, 2020, Proceedings, Part XV 16*, pages 208–223. Springer, 2020. 2, 5
- [31] Zhi Tian, Chunhua Shen, and Hao Chen. Conditional convolutions for instance segmentation. In *Computer Vision—ECCV 2020: 16th European Conference, Glasgow, UK, August 23–28, 2020, Proceedings, Part I 16*, pages 282–298. Springer, 2020. 5, 7
- [32] Liwei Wang, Yin Li, Jing Huang, and Svetlana Lazebnik. Learning two-branch neural networks for image-text matching tasks. *IEEE Transactions on Pattern Analysis and Machine Intelligence*, 41(2):394–407, 2018. 2
- [33] Peng Wang, Qi Wu, Jiewei Cao, Chunhua Shen, Lianli Gao, and Anton van den Hengel. Neighbourhood watch: Referring expression comprehension via language-guided graph attention networks. In *Proceedings of the IEEE/CVF Conference on Computer Vision and Pattern Recognition*, pages 1960–1968, 2019. 2
- [34] Syed Talal Wasim, Muzammal Naseer, Salman Khan, Ming-Hsuan Yang, and Fahad Shahbaz Khan. Videogrounding-dino: Towards open-vocabulary spatio-temporal video grounding. In *Proceedings of the IEEE/CVF Conference on Computer Vision and Pattern Recognition*, pages 18909–18918, 2024. 2
- [35] Jiannan Wu, Yi Jiang, Peize Sun, Zehuan Yuan, and Ping Luo. Language as queries for referring video object segmentation. In *Proceedings of the IEEE/CVF Conference on Computer Vision and Pattern Recognition*, pages 4974–4984, 2022. 1, 2, 6, 7
- [36] Ning Xu, Linjie Yang, Yuchen Fan, Dingcheng Yue, Yuchen Liang, Jianchao Yang, and Thomas Huang. Youtube-vos: A large-scale video object segmentation benchmark. *arXiv preprint arXiv:1809.03327*, 2018. 1
- [37] Linfeng Yuan, Miaoqing Shi, Zijie Yue, and Qijun Chen. Losh: Long-short text joint prediction network for referring video object segmentation. In *Proceedings of the IEEE/CVF Conference on Computer Vision and Pattern Recognition*, pages 14001–14010, 2024. 1, 2, 6, 7
- [38] Hao Zhang, Feng Li, Shilong Liu, Lei Zhang, Hang Su, Jun Zhu, Lionel M Ni, and Heung-Yeung Shum. Dino: Detr with improved denoising anchor boxes for end-to-end object detection. *arXiv preprint arXiv:2203.03605*, 2022. 2
- [39] Xizhou Zhu, Weijie Su, Lewei Lu, Bin Li, Xiaogang Wang, and Jifeng Dai. Deformable detr: Deformable transformers for end-to-end object detection. *arXiv preprint arXiv:2010.04159*, 2020. 4